AIAA 80-0304R

Structural Properties of Superplastically Formed, Diffusion-Bonded Orthogonally Corrugated Core Sandwich Plates

William L. Ko*
NASA Dryden Flight Research Center, Edwards, Calif.

A new orthogonally corrugated sandwich structure that can be fabricated by using the superplastic forming-diffusion bonding (SPF-DB) process is described. Formulas and the associated plots for evaluating the effective elastic constants and the bending stiffnesses for the core of this new sandwich structure are presented. The structural properties of this sandwich structure are compared with the conventional honeycomb core sandwich structure under the condition of equal sandwich density. The SPF-DB orthogonally corrugated sandwich core has higher transverse shear stiffness than the conventional honeycomb sandwich core, but has lower stiffness in the sandwich core thickness direction.

Nomenclature

B = nondimensional geometrical parameter associated with relative displacement δ of two ends of symmetrical corrugation leg
b = $\frac{1}{2}(p-f)$, one half of horizontal projected length of circular arcs and straight diagonal segments of corrugation leg
D = bending stiffness per unit width of sandwich core or solid core
d = one half of the length of straight diagonal segment of corrugation leg
E = modulus of elasticity
F = vertical load in sandwich thickness direction, per unit width in corrugation axis direction, applied at end point of corrugation leg
f = length of corrugation flat segment (crest or trough)
G = shear modulus
H = horizontal load in crest direction, per unit width in corrugation axis direction, applied at end point of corrugation leg
h = depth of sandwich structure or depth of sandwich core
I = $(1/12)t^3$, moment of inertia, per unit width, of cross section of corrugation leg segment of thickness t, with respect to horizontal centroidal axis of cross section
$\hat{I}$ = moment of inertia, per unit width, of unidirectional corrugation cross section normal to corrugation axis, taken about the horizontal centroidal axis of corrugation cross section
l = $f+2d+2R\theta$, length of one corrugation leg
p = one half of corrugation pitch (or half wave length of corrugation)
R = radius of circular arc segments of corrugation leg
t = thickness of sandwich core sheet or sandwich face sheet
x,y,z = Cartesian coordinates
γ = density
δ = displacement of one end of corrugation leg with respect to the other end
θ = corrugation angle (angle between centerline of straight segment and centerline of corrugation flat segment)
ν = Poisson's ratio

Subscripts

HC = honeycomb sandwich core
SP = SPF-DB orthogonally corrugated sandwich core
Ti = titanium
Al = aluminum
[ ] = quantities associated with SPF-DB unidirectionally corrugated sandwich core
[ ]* = quantities associated with SPF-DB orthogonally corrugated sandwich core
[~] = quantities associated with honeycomb sandwich core
c = sandwich core or sandwich core material
s = sandwich face sheets
x,y,z = associated with x, y, z directions

Superscripts

F = application of vertical loads at ends of corrugation leg
H = application of horizontal loads at ends of corrugation leg

Introduction

In recent years, the so-called superplastically formed, diffusion-bonded (SPF-DB) sandwich structures have shown potential for future aerospace application, and could challenge the present use of conventional honeycomb core sandwich structures. The usual process for fabricating the SPF-DB sandwich structure is depicted in Fig. 1. First, component sheets of superplastic alloy (such as titanium) are masked using stop-off films at a selected interfacial area where diffusion bonding is not desired. The component sheets are then solid-state diffusion bonded inside a containment (or die cavity) under high temperature and high pressure. Finally, the diffusion bonded multiple sheet pack is superplastically expanded inside the die cavity by high internal pressure under high temperature to give a desired configuration.[1,2]

Superplasticity is the ability of a material to undergo large plastic deformations [up to 1000% strain for titanium alloys and up to 4850% for an eutectic lead-tin alloy (Pb-62% Sn eutectic)[3]] at high temperatures without localized thinning (or necking). The sandwich structure formed by the SPF-DB process will have "surface" bonding between the face sheets and the sandwich core instead of "line" bonding as in the case of ordinary honeycomb core sandwich structures. The typical

Presented as Paper 80-0304 at the AIAA 18th Aerospace Sciences Meeting, Pasadena, Calif., Jan. 14-16, 1980; submitted March 6, 1980; revision received Aug. 3, 1981. This paper is declared a work of the U.S. Government and therefore is in the public domain.

*Aerospace Engineer, Aeronautical Engineering Division, Structures Branch. Member AIAA.

SPF-DB sandwich core configurations are the unidirectionally corrugated core (including the truss core), sine-wave core (the corrugation axis is sinusoidal), dimpled core (egg-carton type core) and so forth.[2,4-7]

In the unidirectionally corrugated core and the sine-wave core, the bending and transverse shear stiffnesses are quite high in the direction of the corrugation axis but very low in the direction normal to the corrugation axis. The dimpled core has relatively low out-of-plane bending and transverse shear stiffnesses in any in-plane direction. In order to eliminate these structural shortcomings, the author proposes a new type of SPF-DB sandwich core: the "orthogonally corrugated" sandwich core. The new type of sandwich core consists of two families of unidirectional corrugations mutually intersecting in the same plane at an angle of 90 deg. The advantage of this new core is that it offers not only the high out-of-plane bending and transverse shear stiffness, but it also carries a considerable share of in-plane normal loadings and edgewise shear loadings.

The purpose of this paper is to calculate the effective elastic constants and the bending stiffnesses for the orthogonally corrugated SPF-DB sandwich core, and to present graphs for evaluating the elastic constants and the bending stiffnesses. These graphs can be used in the comparison of the structural advantages of SPF-DB orthogonally corrugated core and conventional honeycomb core.

SPF-DB Orthogonally Corrugated Sandwich Panel

The four superplastic alloy component sheets used in the fabrication of the SPF-DB orthogonally corrugated core sandwich panel are shown in Fig. 2. The interfacial bonding regions and the interfacial bonding-stopoff regions are shown clearly. In the upper and lower core sheets, small pressure gas passing holes are arrayed in such a way that during the superplastic expansion of the core under internal pressure, the pressure gas can penetrate to every core cell (or compartment).

The SPF-DB expansion process for fabricating the orthogonally corrugated core sandwich panel is shown in Fig. 1. The pile of the four component sheets with stopoffs inserted at the interfaces (Fig. 1a) are first diffusion bonded inside the die cavity under gas pressures at an elevated temperature (Fig. 1b). Then the diffusion-bonded multiple-sheet pack is expanded superplastically inside the die cavity under internal pressure at a high temperature (Fig. 1c). For superplastic alloys such as titanium, the temperatures for diffusion bonding and for superplastic forming are the same.[2] The final expanded configuration of the SPF-DB orthogonally corrugated core sandwich panel is shown in Fig. 3. The core of this sandwich structure actually consists of a square array of inverted, hollow, truncated pyramids (formed from the upper core sheet), staggered and joined together with another square array of upright, hollow, truncated pyramids (formed from the lower core sheet) at the edges of their triangular sides. The resulting orthogonally intersecting corrugated core can be optimized to one of the high-efficiency structures that can be generated by using the SPF-DB process.

In the analysis, both families of intersecting corrugations are identical symmetrical corrugations, and the corrugation leg consists of two flat segments, two circular arc segments, and a straight diagonal segment (Fig. 3). The effect of pressure gas passing holes is neglected.

Elastic Constants for SPF-DB Orthogonally Corrugated Sandwich Core

For the case when the planar dimensions (that is, in the x and y directions) of the SPF-DB orthogonally corrugated sandwich plate are many times the corrugation pitch, the sandwich core can be represented by an equivalent continuum material. The elastic constants evaluated in the following are the effective elastic constants pertaining to this equivalent continuum sandwich core.

The effective elastic constants for the SPF-DB unidirectionally corrugated sandwich core are determined in Refs. 6 and 7. By use of the principle of superposition the results of Refs. 6 and 7 can be used to construct most of the effective

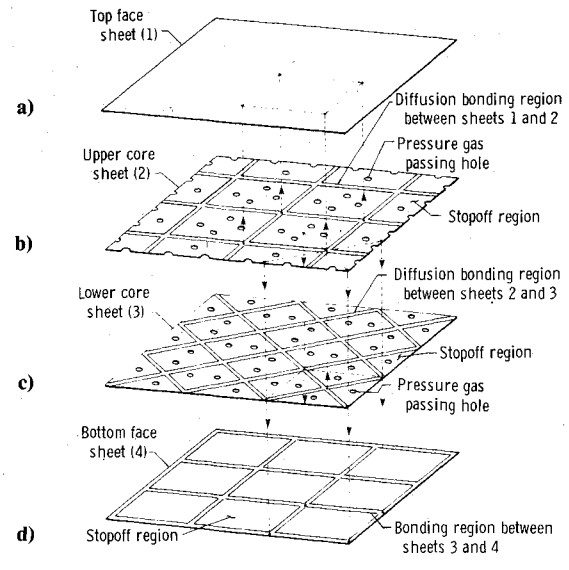

Fig. 1 Superplastic forming, diffusion-bonding expansion process.

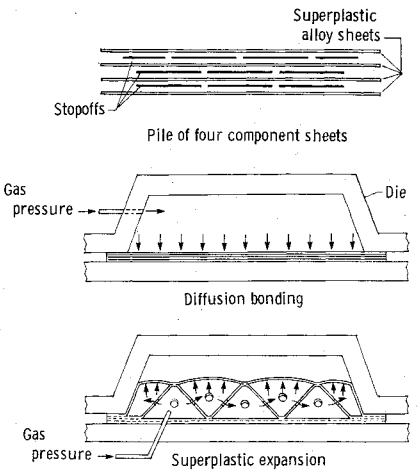

Fig. 2 Component sheets for superplastically formed, diffusion-bonded orthogonally corrugated core sandwich panel.

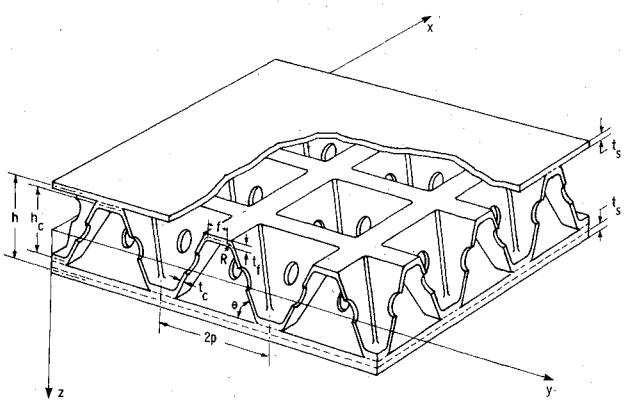

Fig. 3 Geometry of superplastically formed, diffusion-bonded orthogonally corrugated core sandwich plate.

elastic constants for the SPF-DB orthogonally corrugated sandwich core. Let [ ] and [ ]*, respectively, denote the effective elastic constants for the unidirectionally and the orthogonally corrugated sandwich cores. Then

$$E_x^*=E_y^*=E_x+E_y \tag{1}$$

where

$$E_x+E_y=E_c\frac{t_f}{h_c}+E_c\frac{I_c p}{B_y^H h_c^4}\approx E_c\frac{t_f}{h_c}\quad(E_x\gg E_y) \tag{2}$$

$$G_{xy}^*=2G_{xy}=2G_c\frac{p^2 t_f}{l^2 h_c} \tag{3}$$

$$G_{yz}^*=G_{zx}^*=G_{yz}+G_{zx} \tag{4}$$

where

$$G_{yz}+G_{zx}=\frac{E_c I_c}{h_c^3\left(\frac{h_c}{p}B_z^F-2B_z^H+\frac{p}{h_c}B_y^H\right)}+G_c\frac{h_c t_f}{l^2} \tag{5}$$

$$\nu_{xy}^*=\nu_{yx}^*=\nu_{zx}^*=\nu_{zy}^*=\nu_c \tag{6}$$

$$\nu_{xz}^*=\nu_{yz}^*=\nu_{xz}=\frac{\nu_c}{B_z^F}\frac{I_c}{h_c t_c l}\ll 1 \tag{7}$$

The symbols B_y^H, B_z^H, B_y^F, and B_z^F in Eqs, (2), (5), and (7) are the nondimensional geometrical prameters associated with corrugation leg end displacements δ_y^H, δ_z^H, δ_y^F, and δ_z^F, respectively (see Fig. 4), and are defined as

$$B_y^H=\frac{2}{3}\left(\frac{d}{h_c}\right)^3\sin^2\theta+\frac{1}{2}\left(\frac{R}{h_c}\theta+\frac{1}{2}\frac{f}{h_c}\frac{I_c}{I_f}\right)$$
$$-\left(\frac{R}{h_c}\right)^2\left[\left(2-3\frac{R}{h_c}\right)(\theta-\sin\theta)+\frac{R}{h_c}\sin\theta(1-\cos\theta)\right]$$
$$+\frac{I_c}{h_c^2 t_c}\left[\frac{f}{h_c}\frac{t_c}{t_f}+2\frac{d}{h_c}\cos^2\theta+\frac{R}{h_c}(\theta+\sin\theta\cos\theta)\right] \tag{8}$$

$$B_z^H=\frac{2}{3}\left(\frac{d}{h_c}\right)^3\sin\theta\cos\theta+\frac{1}{2}\frac{I_c}{I_f}\left[\frac{1}{4}\left(\frac{p}{h_c}\right)^2-\left(\frac{b}{h_c}\right)^2\right]$$
$$+\frac{R}{h_c}\left\{\frac{b}{h_c}\theta-2\frac{Rb}{h_c^2}(\theta-\sin\theta)\right.$$
$$\left.-\frac{R}{h_c}(1-\cos\theta)\left[1-\frac{R}{h_c}(1-\cos\theta)\right]\right\}$$
$$-\frac{I_c}{h_c^2 t_c}\left(2\frac{d}{h_c}\sin\theta\cos\theta+\frac{R}{h_c}\sin^2\theta\right)=B_y^F \tag{9}$$

$$B_z^F=\frac{2}{3}\left(\frac{d}{h_c}\right)^3\cos^2\theta+\frac{2}{3}\frac{I_c}{I_f}\left[\frac{1}{8}\left(\frac{p}{h_c}\right)^3-\left(\frac{b}{h_c}\right)^3\right]$$
$$+\frac{R}{h_c}\left[2\left(\frac{b}{h_c}\right)^2\theta-4\frac{Rb}{h_c^2}(1-\cos\theta)+\left(\frac{R}{h_c}\right)^2(\theta-\sin\theta\cos\theta)\right]$$
$$+\frac{I_c}{h_c^2 t_c}\left[2\frac{d}{h_c}\sin^2\theta+\frac{R}{h_c}(\theta-\sin\theta\cos\theta)\right] \tag{10}$$

The remaining modulus of elasticity E_z^* in the z direction is calculated as follows. If the corrugation leg $00'$ is not constrained by the transverse corrugation 0A0′B, then under the vertical loading F (per unit width in the z direction) point 0 will move to point 0_1 (see Fig. 4). The horizontal and vertical components of the displacement $\overline{00_1}$, δ_y^F and δ_z^F, are given in Eqs. (27) and (21), respectively, of Ref. 6

$$\delta_y^F=[(Fh_c^3)/(E_c I_c)]B_y^F \tag{11}$$

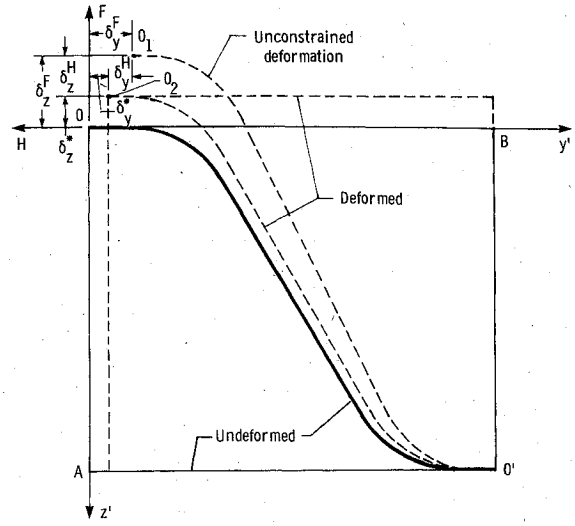

Fig. 4 Deformation of orthogonally intersecting corrugation leg unit.

$$\delta_z^F=[(Fh_c^3)/(E_c I_c)]B_z^F \tag{12}$$

Because of the constraint of the transverse corrugation 0A0′B, point 0 can only move to point 0_2. The effect of the transverse constraint can be achieved by pulling point 0 back from position 0_1 to position 0_2 with the application of a horizontal loading H (per unit width in the x direction). The horizontal and vertical components of the displacement $0_1 0_2$, δ_y^H, and δ_z^H, are given by Eqs. (11) and (16), respectively, of Ref. 6 in the following forms:

$$\delta_y^H=[(Hh_c^3)/(E_c I_c)]B_y^H \tag{13}$$

$$\delta_z^H=[(Hh_c^3)/(E_c I_c)]B_z^H \tag{14}$$

The horizontal component of the displacement $\overline{00_2}$, δ_y^*, is due to the Poisson's effect of the transverse corrugation 0A0′B and can be calculated easily as follows:

$$\delta_y^*=(F\nu_c' h_c p)/(l t_c E_c) \tag{15}$$

From the relation

$$\delta_y^*=\delta_y^F-\delta_y^H \tag{16}$$

it is possible to relate H to F in the light of Eqs. (11), (13), and (15) by

$$H=F[B_y^F/B_y^H-(\nu_c I_c p)/(l t_c h_c^2 B_y^H)] \tag{17}$$

From Eqs. (12), (14), and (17), the vertical component of the displacement 00_2, δ_z^*, can be written as

$$\delta_z^*=\delta_z^F-\delta_z^H \tag{18}$$

$$=\frac{Fh_c^3 B_z^F}{E_c I_c}\left[1-\frac{B_z^H B_y^F}{B_y^H B_z^F}\left(1-\frac{B_z^F p}{B_y^F h_c}\frac{\nu_c I_c}{l t_c h_c B_z^F}\right)\right] \tag{19}$$

Because there are two corrugations in the unit cell, the actual vertical displacement of point 0 will be $\delta_z^*/2$.

The modulus of elasticity E_z^* can then be expressed as follows:

$$E_z^*=\frac{F}{p}\Big/\left(\frac{\delta_z^*}{2}\frac{1}{h_c}\right) \tag{20}$$

$$=2E_z\Big/\left[1-\nu_{yz}\nu_{zy}\left(1-\frac{\nu_{xz}}{\nu_{yz}}\right)\right] \tag{21}$$

utilizing the following relationships:

$$\nu_{yz}=\frac{h_c}{p}\frac{B_y^F}{B_z^F},\quad \nu_{zy}=\frac{p}{h_c}\frac{B_z^H}{B_y^H},\quad \nu_{xz}=\frac{\nu_c}{B_z^F}\frac{I_c}{h_c t_c l} \tag{22}$$

which are given in Refs. 6 and 7. The factor[2] appearing in Eq. (21) is caused by the two orthogonally intersecting corrugations. Because $\nu_{xz}\approx 0$, Eq. (21) can be simplified to

$$E_z^*=2E_z/(1-\nu_{yz}\nu_{zy}) \tag{23}$$

This equation also applies when the core is bonded to the surface sheets.

Corrugated Core Bending Stiffness

The bending stiffness in the x or y direction of the SPF-DB orthogonally corrugated sandwich core is practically the same as the bending stiffness in the x direction of the SPF-DB unidirectionally corrugated sandwich core (see Fig. 1 of Ref. 6 or 7) because one family of the orthogonal corrugations, which is transverse to the direction of bending, has negligible bending stiffness compared with the other family, which is parallel to the direction of bending.

If D_x^* and D_y^* denote the bending stiffnesses, per unit width, of beams cut from the SPF-DB orthogonally corrugated core in the x and y directions, respectively, then

$$D_x^*=D_y^*\approx D_x=E_c\hat{I} \tag{24}$$

where D_x is the bending stiffness, per unit width, of a beam cut from the SPF-DB unidirectionally corrugated core in the x direction[6,7] and

$$\hat{I}=\frac{h_c^3 t_c}{p}\left\{\frac{1}{4}\frac{f}{h_c}\frac{t_f}{t_c}\left(1+\frac{1}{3}\frac{t_f^2}{h_c^2}\right)+\frac{2}{3}\frac{d^3}{h_c^3}\left(\sin^2\theta+\frac{1}{4}\frac{t_c^2}{d^2}\cos^2\theta\right)\right.$$
$$\left.+\frac{R}{h_c}\left[\frac{\theta}{2}-2\frac{R^2}{h_c^2}\sin\theta-\frac{R}{h_c}\left(2-3\frac{R}{h_c}\right)(\theta-\sin\theta)\right]\right\} \tag{25}$$

which is the moment of inertia, per unit width, of the unidirectional corrugation cross section parallel to the yz plane (see Fig. 1 of Ref. 6 or 7), taken about the horizontal centroidal axis of the corrugation cross section.

If face sheets are present, the contribution of the bending stiffness (per unit width of a beam cut from the sandwich plate) from the two identical face sheets is $\frac{1}{2}E_s t_s h^2$, where

E_s = modulus of elasticity of the surface sheets (E_s is generally equal to E_c for the SPF-DB sandwich structures)
t_s = thickness of the surface sheets
$h=h_c+2t_f+t_s$, distance between the middle surfaces of the face sheets

Numerical Results

In the generation of graphs for evaluating the major elastic constants and the bending stiffnesses for SPF-DB orthogonally corrugated sandwich cores, the core material is titanium 6A1-4V alloy having the following physical properties, which are denoted by $(\,)_{\mathrm{Ti}}$:

$E_c=E_{\mathrm{Ti}}=11.0316\times10^{10}$ N/m^2 (16×10^6 psi)
$G_c=G_{\mathrm{Ti}}=4.2747\times10^{10}$ N/m^2 (6.2×10^6 psi)
$\nu_c=\nu_{\mathrm{Ti}}=0.33$
$\gamma_c=\gamma_{\mathrm{Ti}}=4.47$ g/cm^3 (0.16 lb/in.^{3})

Graphs for evaluating the modulus of elasticity E_z^* are shown in Fig. 5. For a given corrugation crest thickness t_f/h_c, E_z^* is quite sensitive to the changes of both half-corrugation pitch p/h_c and the corrugation angle θ, and E_z^* reaches its optimum value when the corrugation crest length becomes zero ($f=0$; that is, a triangular truss core). The "envelopes of optimum points" shown in Fig. 5 correspond to the case when the crest length tends to zero ($f=0$).

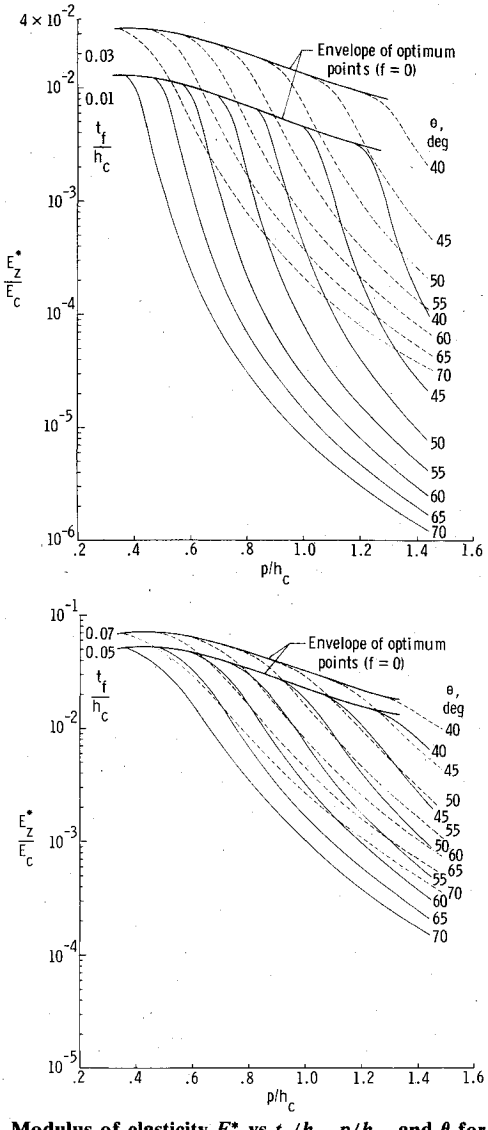

Fig. 5 Modulus of elasticity E_z^* vs t_f/h_c, p/h_c, and θ for SPF-DB orthogonally corrugated sandwich core; $R=t_f$, $\nu_c=0.33$.

The variation of shear modulus G_{xy}^* with t_f/h_c and θ is shown in Fig. 6. The "envelopes of limit points" shown in the figure correspond to the triangular truss core. For a given t_f/h_c and θ, the triangular truss core has the lowest value of G_{xy}^*.

The transverse shear modulus G_{yz}^* ($=G_{zx}^*$) is quite sensitive to t_f/h_c, p/h_c, and θ (see Fig. 7). The triangular truss core has the highest value of G_{yz}^*. We note that a slight increase of the crest length f from 0 (that is, slight deviation from the triangular truss core into a trapesoidal truss core) will drastically lower the value of G_{yz}^*.

The bending stiffness D_x^* ($=D_y^*$), which is normalized by $D_c=E_c(h_c^3/12)$ (the bending stiffness, per unit width, of a solid beam with a depth h_c, made of material with the modulus of elasticity E_c) is plotted in Fig. 8. The triangular truss core appears to have the lowest bending stiffness. This low bending stiffness is expected because, for a finite value of f, the crest and trough will act as flanges in resisting the bending. Thus, if the bending stiffness D_x^* is to be increased by increasing f, the shear stiffness G_{yz}^* has to be sacrificed (see Fig. 7). Therefore, careful choice of the value of f is essential in optimizing the sandwich core structure properties.

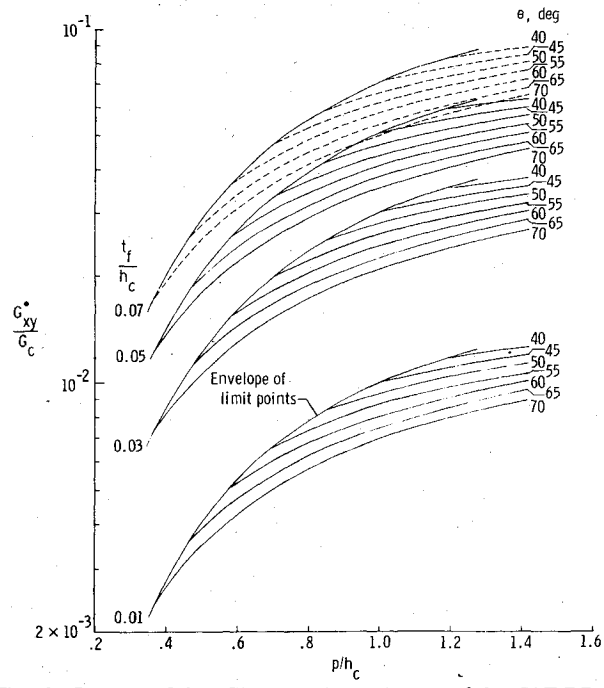

Fig. 6 Shear modulus G^*_{xy} vs t_f/h_c, p/h_c, and θ for SPF-DB orthogonally corrugated sandwich core; $R=t_f$.

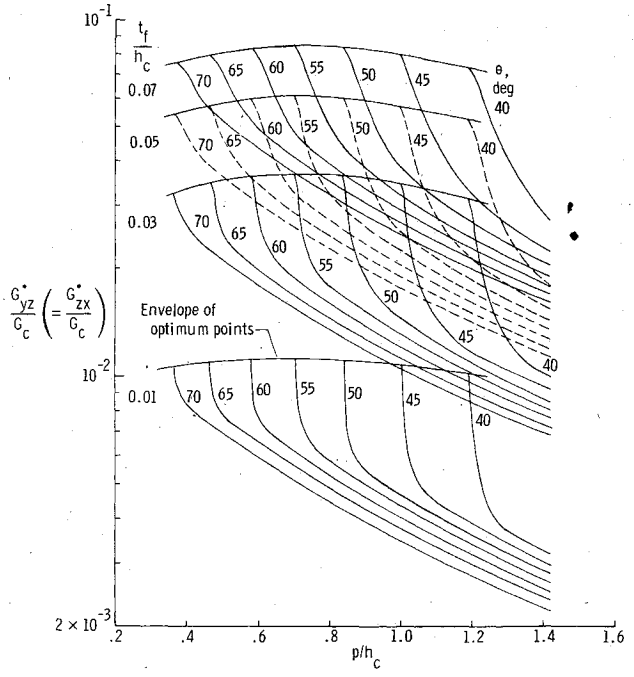

Fig. 7 Shear modulus G^*_{yz} $(=G^*_{zx})$ vs t_f/h_c, p/h_c, and θ for SPF-DB orthogonally corrugated sandwich core; $R=t_f$.

Comparison with Honeycomb Sandwich Core

The comparison of stiffness of the SPF-DB orthogonally corrugated sandwich core and the honeycomb sandwich core is based on the condition that both types of sandwich cores have the same density and the same core depths. The SPF-DB orthogonally corrugated core chosen for comparison has right triangular corrugations (i.e., $\theta=60$ deg, $f=0$, a high stiffness configuration). The elastic constraints E^*_z, G^*_{xy}, G^*_{yz} $(=G^*_{zx})$, and the bending stiffness D^*_x $(=D^*_y)$ for this typical configuration are obtained from Figs. 5 to 8 and are plotted against the corrugation crest thickness t_f/h_c in Fig. 9. The honeycomb core (see Fig. 10) picked for comparison is a

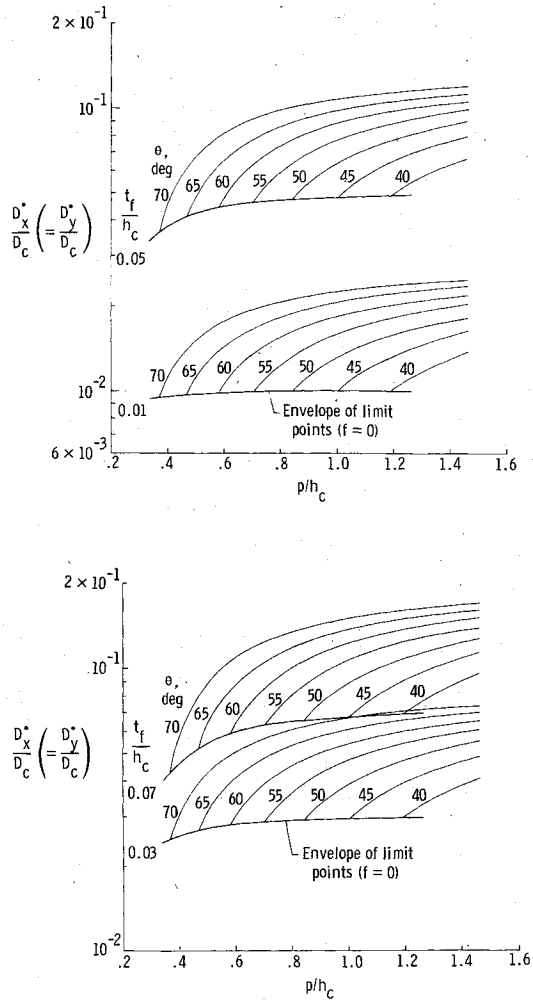

Fig. 8 Bending stiffness D^*_x $(=D^*_y)$ vs t_f/h_c, p/h_c, and θ for SPF-DB orthogonally corrugated sandwich core; $R=t_f$.

typical one used in high-speed aircraft and has the following geometrical parameters:

$$(t_f/h_c)_{HC}=0.0147, \quad (f/h_c)_{HC}=0.4053 \tag{26}$$

$$(p/h_c)_{HC}=0.9825, \quad (l/h_c)_{HC}=1.5600, \quad (\theta)_{HC}=60 \text{ deg} \tag{27}$$

The material used for the honeycomb sandwich core can be either titanium or aluminum. For aluminum, the following physical properties, denoted by $(\,)_{Al}$, are used:

$$E_c=E_{Al}=6.8948\times10^{10} \text{ N/m}^2 \ (10\times10^6 \text{ psi})$$
$$G_c=G_{Al}=2.7579\times10^{10} \text{ N/m}^2 \ (4\times10^6 \text{ psi})$$
$$\nu_c=\nu_{Al}=0.36$$
$$\gamma_c=\gamma_{Al}=2.77 \text{ g/cm}^3 \ (0.100 \text{ lb/in.}^3)$$

The honeycomb sandwich core is made up of numerous unidirectionally corrugated strips joined together at the corrugation flat segments, with corrugation axis oriented normal to the sandwich middle surface (see Fig. 10). Therefore, the effective elastic constants $\tilde{E}_z$, $\tilde{G}_{yz}$, and $\tilde{G}_{zx}$ of the honeycomb sandwich core can be obtained easily from Ref. 6 or 7 if the coordinate system in Fig. 1 of Ref. 6 or 7 is changed to fit the coordinate system in Fig. 10, and if the core sheet thickness is uniform (i.e., $t_c=t_f$). The honeycomb sandwich core bending stiffnesses $\tilde{D}_x$ and $\tilde{D}_y$ can be calculated easily from the following formulas:

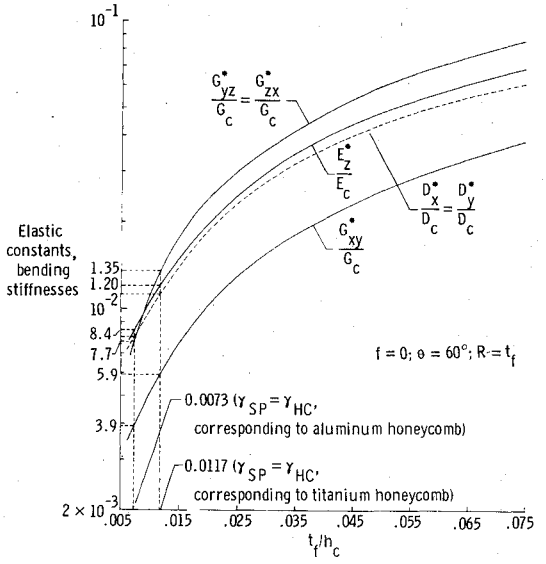

Fig. 9 Elastic constants and bending stiffnesses vs t_f/h_c for SPF-DB orthogonally corrugated sandwich core.

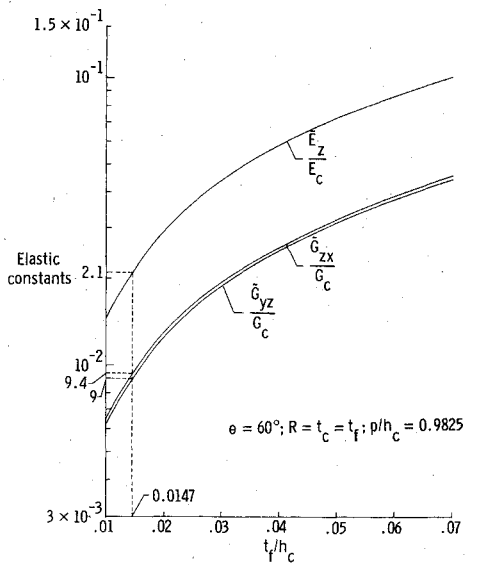

Fig. 11 Elastic constants vs t_f/h_c for honeycomb sandwich core.

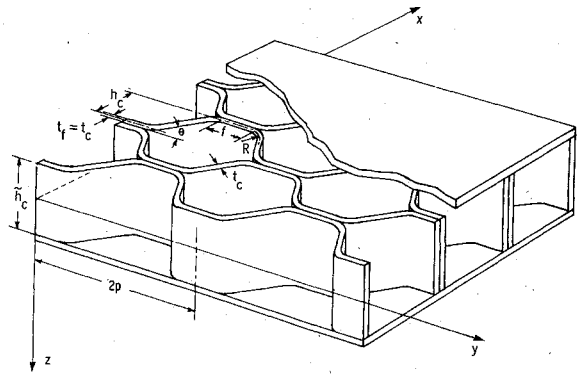

Fig. 10 Geometry of honeycomb core sandwich plate.

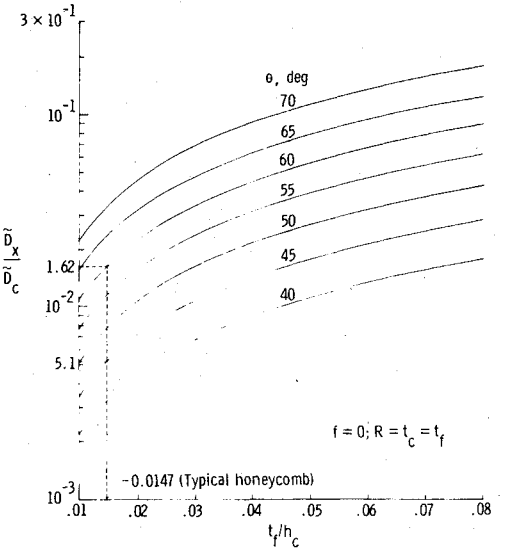

Fig. 12 Bending stiffness $\tilde{D}_x$ vs t_f/h_c and θ for honeycomb core.

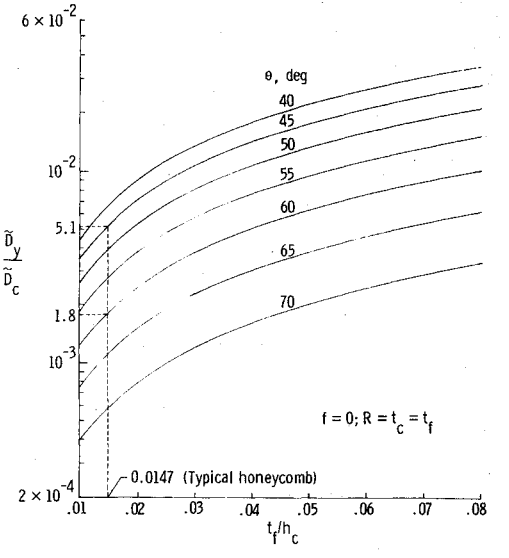

Fig. 13 Bending stiffness $\tilde{D}_y$ vs t_f/h_c and θ for honeycomb core.

$$\tilde{D}_x = \frac{\tilde{h}^3}{12}\frac{E_x}{1-\nu_{yx}\nu_{xy}} \tag{28}$$

$$\tilde{D}_y = \frac{\tilde{h}^3}{12}\frac{E_y}{1-\nu_{xy}\nu_{yx}} \tag{29}$$

where $\tilde{h}$ is the depth of the honeycomb sandwich core (see Fig. 10); E_x, E_y are the effective moduli of elasticity; and ν_{xy}, ν_{yx} are the effective Poisson's ratios of the unidirectionally corrugated core, all of which can be found from Ref. 6 or 7. $\tilde{E}_z$, $\tilde{G}_{yz}$, $\tilde{G}_{zx}$ for corrugation angle $\theta = 60$ deg, and the bending stiffnesses $\tilde{D}_x$, $\tilde{D}_y$ are plotted against the sandwich core thickness t_f/h_c for a condition $(p/h_c)_{HC} = 0.9825$ [Eq. (27)] and are shown in Figs. 11-13. In the plots, both $\tilde{D}_x$ and $\tilde{D}_y$ are normalized by $\tilde{D}_c = E_c(\tilde{h}^3/12)$, the bending stiffness, per unit width, of a solid beam with depth $\tilde{h}$ made of material with modulus of elasticity E_c. Because $\tilde{D}_x$ is independent of f and $\tilde{D}_y$ is insensitive to the change of f, in plotting Figs. 12 and 13, f is set to zero.

Let $(\,)_{SP}$ and $(\,)_{HC}$ denote the quantities associated with the SPF-DB orthogonally corrugated sandwich core and the honeycomb sandwich core, respectively. The density of the SPF-DB orthogonally corrugated core γ_{SP} can be written as

$$\gamma_{SP} = 2(t_f/h_c)_{SP}\gamma_{Ti} \tag{30}$$

and the density γ_{HC} of the honeycomb core can be written as

$$\gamma_{HC} = [(t_c l)/(h_c p)]_{HC}\gamma_c \tag{31}$$

Table 1 Elastic constants and bending stiffnesses for titanium honeycomb core and for SPF-DB titanium orthogonally corrugated core ($\gamma_{SP} = \gamma_{HC}$)

Titanium honeycomb core[a]		SPF-DB titanium orthogonally corrugated core[b]		$()_{SP}/()_{HC}$
	$\theta = 60$ deg			
$\bar{E}_z$, N/m^2 (psi)	23.17×10^8 (33.60×10^4)	E_z^*, N/m^2 (psi)	13.20×10^8 (19.20×10^4)	0.57
$\bar{G}_{yz}$, N/m^2 (psi)	3.85×10^8 (5.58×10^4)	G_{yz}^*, N/m^2 (psi)	4.39×10^8 (6.37×10^4)	1.14
$\bar{G}_{zx}$, N/m^2 (psi)	4.02×10^8 (5.83×10^4)	G_{zx}^*, N/m^2 (psi)	4.39×10^8 (6.37×10^4)	1.09
$\bar{D}_x$, N/m (in./lb)	24.41×10^2 (21.60×10^3)	D_x^*, N/m (in./lb)	17.02×10^2 (15.07×10^3)	0.70
$\bar{D}_y$, N/m (in./lb)	2.71×10^2 (2.40×10^3)	D_y^*, N/m (in./lb)	17.02×10^2 (15.07×10^3)	6.28
$\theta = 45$ deg		$\theta = 60$ deg		
$\bar{D}_x$, $\bar{D}_y$, N/m (in./lb)	7.68×10^2 (6.80×10^3)	D_x^*, D_y^*, N/m (in./lb)	17.02×10^2 (15.07×10^3)	2.22

[a] $t_f/h_c = 0.0147$, $f/h_c = 0.4053$, $\bar{h} = 2.54\times10^{-2}$ m (1 in.). [b] $t_f/h_c = 0.0117$, $f/h_c = 0$, $h_c = 2.54\times10^{-2}$ m (1 in.).

Table 2 Elastic constants and bending stiffnesses for aluminum honeycomb core and SPF-DB titanium orthogonally corrugated core ($\gamma_{SP} = \gamma_{HC}$)

Aluminum honeycomb core[a]		SPF-DB titanium orthogonally corrugated core[b]		$()_{SP}/()_{HC}$
	$\theta = 60$ deg			
$\bar{E}_z$, N/m^2 (psi)	14.48×10^8 (21.00×10^4)	E_z^*, N/m^2 (psi)	9.27×10^8 (13.44×10^4)	0.64
$\bar{G}_{yz}$, N/m^2 (psi)	2.48×10^8 (3.60×10^4)	G_{yz}^*, N/m^2 (psi)	3.25×10^8 (4.71×10^4)	1.31
$\bar{G}_{zx}$, N/m^2 (psi)	2.59×10^8 (3.76×10^4)	G_{zx}^*, N/m^2 (psi)	3.25×10^8 (4.71×10^4)	1.25
$\bar{D}_x$, N/m (in./lb)	15.25×10^2 (13.50×10^3)	D_x^*, N/m (in./lb)	12.05×10^2 (10.67×10^3)	0.79
$\bar{D}_y$, N/m (in./lb)	1.69×10^2 (1.50×10^3)	D_y^*, N/m (in./lb)	12.05×10^2 (10.67×10^3)	7.13
$\theta = 45$ deg		$\theta = 60$ deg		
$\bar{D}_x$, $\bar{D}_y$, N/m (in./lb)	4.80×10^2 (4.25×10^3)	D_x^*, D_y^*, N/m (in./lb)	12.05×10^2 (10.67×10^3)	2.51

[a] $t_f/h_c = 0.0147$, $f/h_c = 0.4053$, $\bar{h} = 2.54\times10^{-2}$ m (1 in.). [b] $t_f/h_c = 0.0073$, $f/h_c = 0$, $h_c = 2.54\times10^{-2}$ m (1 in.).

For the equal-density condition $\gamma_{SP} = \gamma_{HC}$, Eqs. (30) and (31) can be combined to give the relationship between the geometrical parameters of the two types of sandwich cores

$$\left(\frac{t_f}{h_c}\right)_{SP} = \frac{l}{2}\left(\frac{t_c l}{p h_c}\right)_{HC}\frac{\gamma_c}{\gamma_{Ti}} \tag{32}$$

With Eq. (32), the given honeycomb sandwich core geometries [Eqs. (26) and (27)], and the given material properties, the crest thickness of the SPF-DB orthogonally corrugated sandwich core can be determined as

$$(t_f/h_c)_{SP} = 0.0117 \tag{33}$$

which corresponds to titanium honeycomb sandwich core $[(t_f/h_c)_{HC} = 0.0147]$, or

$$(t_f/h_c)_{SP} = 0.0073 \tag{34}$$

which corresponds to aluminum honeycomb sandwich core $[(t_f/h_c)_{HC} = 0.0147]$. Conditions given in Eqs. (26), (33), and (34) can then be used to find from Figs. 9 and 11-13 proper values of effective elastic constants and the bending stiffnesses of the two types of sandwich cores. The results are shown in Tables 1 and 2. The values of the bending stiffnesses in the tables are for the sandwich core depth of 2.54 cm (1 in.). Notice that in Tables 1 and 2 the bending stiffnesses for two cases of honeycomb sandwich core configurations (i.e., $\theta = 60$ and 45 deg) are shown. In the comparison of structural properties, the corrugation angles θ for the two types of sandwich cores do not have to be equal. The SPF-DB orthogonally corrugated core has higher transverse shear stiffness than the honeycomb core (titanium or aluminum), but is less stiff in the sandwich thickness direction. We also notice that the moduli of elasticity E_z^* and $\bar{E}_z$ are quite small (compared with the solid core) and cannot be regarded as infinite as in conventional plate analysis. Because of these low values, swelling modes of vibrations (where the two face sheets oscillate in opposite directions) could be excited under aerospace service conditions (such as jet noise and high-frequency flutter) and cause fatigue cracks to grow at the face-sheet/core bonding sites. The value of bending stiffness D_x^* $(= D_y^*)$ in the tables is about 16-18% of the bending stiffness of the face sheets if t_s equals t_f and the two face sheets are set apart by 2.54 cm (1 in.).

Concluding Remarks

The geometry and fabrication process of a new SPF-DB orthogonally corrugated sandwich core is discussed, and the formulas and associated graphs for evaluating the major elastic constants and bending stiffnesses of this new sandwich

core are presented. If the length of the crest or trough is increased, the bending stiffness of the sandwich core can be improved; however, the transverse shear stiffness is greatly reduced. For the same sandwich core densities and the same sandwich core depths, the SPF-DB orthogonally corrugated sandwich core with right triangular corrugations has higher transverse shear stiffness than the conventional honeycomb sandwich core (titanium or aluminum), but has lower stiffness in the sandwich core thickness direction.

References

[1] Weisert, E. D., Stacher, G. W., and Kim, B. W., "Manufacturing Methods for Superplastic Forming/Diffusion Bonding Process," Air Force Materials Lab., Wright-Patterson AFB, AFML-TR-79-4053, May 1979.

[2] Pulley, J., "Evaluation of Low-Cost Titanium Structure for Advanced Aircraft," NASA CR-145111, 1976.

[3] Ahmed, M.M.I. and Langdon, T. G., "Exceptional Ductility in the Superplastic Pb-62 Percent Sn Eutectic," *Metallurgical Transactions A*, Vol. 8A, Nov. 1977, pp. 1832-1833.

[4] Ueng, C.E.S., "Superplastically Formed New Sandwich Cores," *Transportation Engineering Journal*, ASME, Vol. 104, July 1978, pp. 437-447.

[5] Ueng, C.E.S., Underwood, E.E., and Liu, T. L., "Shear Modulus of Superplasticity Formed Sandwich Cores," *Trends in Computerized Structural Analysis and Synthesis*, Pergamon Press, New York, 1978, pp. 393-397.

[6] Ko, W. L., "Elastic Constants for Superplastically Formed/Diffusion-Bonded Sandwich Structures," *AIAA Journal*, Vol. 18, Aug. 1980, pp. 986-987.

[7] Ko, W. L., "Elastic Constants for Superplastically Formed/Diffusion-Bonded Corrugated Sandwich Core," NASA TP-1562, May 1980.